Food & Function

ROYAL SOCIETY OF CHEMISTRY

PAPER

View Article Online
View Journal

Cite this: DOI: 10.1039/d0fo00037j

Dihydrochalcones in *Malus* inhibit bacterial growth by reducing cell membrane integrity†

Jinxiao Wang, Ruijia Yang, Zhengcao Xiao, Qipeng Xu, Pengmin Li * and Fengwang Ma

In recent years, increasing research has evaluated the use of natural products as antimicrobial food additives. In this study, antibacterial activity was evaluated for six dihydrochalcone compounds from *Malus*. Phloretin and 3-hydroxyphloretin exhibited antibacterial effects on both Gram-positive and Gram-negative bacteria, and the antibacterial capacity of these compounds was greater than that of their glycosylated derivatives. Within a certain range, dihydrochalcone hydrophobicity was positively correlated with antibacterial activity. Additionally, glycosylation at the 2′-position of the A-ring and hydroxyl group at the 3-position of the B-ring played a key role in the antibacterial activity of dihydrochalcones. Phloretin and 3-hydroxyphloretin caused damage to bacterial cells by significantly increasing protein and inorganic phosphate leakage. Compared to phloretin, 3-hydroxyphloretin exhibited a smaller effect on Gram-positive *Micrococcus luteus* and a greater effect on Gram-negative *Klebsiella pneumoniae*, suggesting different antibacterial mechanisms. At a low dihydrochalcone concentration, the respiration of *M. luteus* did not change, while membrane permeability increased significantly. These results indicate that the antibacterial mechanism of *M. luteus* was primarily damage to the cell membrane. However, damage to respiration and the cell membrane might occur simultaneously in *K. pneumoniae*, suggesting that the antibacterial mechanism of dihydrochalcones also depends on strain type. This study demonstrated the broad-spectrum antibacterial properties of dihydrochalcone compounds commonly found in the genus *Malus* to foodborne pathogens and elucidated the antibacterial mechanisms. It provides theoretical guidance for future research and application of dihydrochalcones in the food industry.

Received 6th January 2020,
Accepted 1st July 2020

DOI: 10.1039/d0fo00037j

rsc.li/food-function

1. Introduction

Flavonoids, possessing a diphenylpropane (C_6–C_3–C_6) skeleton, are widely distributed in plants and occur in the human diet. Besides their positive biofunctions in plants,[1–3] flavonoids may exert protective effects against various disease conditions, including cardiovascular diseases, diabetes, and cancers in humans.[4–7] As bioactive compounds, flavonoids also possess anti-oxidative, antibacterial, and anti-inflammatory properties, among others.[8–11] The antibacterial effects of flavonoids have been studied widely to explore their potential utilization in the food industry as additives.[12] The following mechanisms have been proposed: cytoplasmic membrane damage caused by perforation[13] and/or a change in membrane fluidity resulting from altered membrane composition,[8] the inhibition of nucleic acid synthesis[14] caused by topoisomerase inhibition,[15] and the inhibition of energy metabolism.[16] In general, the antibacterial activity of flavonoids is related to their structure; the number and position of methylation, hydroxyl groups, glycosylation, and prenyl groups can change the antimicrobial activity of flavonoid aglycones.[17–20]

Dihydrochalcones are a unique and important subgroup of flavonoids in apple compared with other fruits.[21–23] Phlorizin, the major dihydrochalcone compound in apple, accounts for 60%–90% of the total flavonoids.[24] Dihydrochalcones have a basic C_6–C_3–C_6 skeleton chemical structure. The A-ring and B-ring are not directly linked like most flavonoids, but are instead linked with a flexible C_3 chain. The flexible molecular structure of dihydrochalcones may result in different properties compared to other flavonoids. For instance, it is generally accepted that an *o*-dihydroxyl group adds to the antioxidant capacity of flavonoids, while *O*-glycosylation reduces it.[25] However, the antioxidant capacities of dihydrochalcone compounds 3-hydroxyphloretin and 3-hydroxytrilobatin (with an *o*-dihydroxyl group at the B-ring) were lower than that of phloretin and trilobatin (without an *o*-dihydroxyl group at the B-ring). Glycosylation at the 2′-position of 3-hydroxyphloretin could increase antioxidant capacity.[26]

State Key Laboratory of Crop Stress Biology for Arid Areas/Shaanxi Key Laboratory of Apple, College of Horticulture, Northwest A&F University, Yangling, Shaanxi 712100, China. E-mail: Lipm@nwsuaf.edu.cn; Fax: +86 29 87082648; Tel: +86 29 87082648

†Electronic supplementary information (ESI) available. See DOI: 10.1039/d0fo00037j

It has been suggested that phloretin and phloridzin (phloretin 2′-*O*-glucoside), the predominant dihydrochalcone compounds in apple and apple-derived products,[27] possess antibacterial capacity through inhibiting the activities of energy metabolism enzymes, such as lactate dehydrogenase and isocitrate dehydrogenase.[16] However, other dihydrochalcone compounds in addition to phloretin and phloridzin have been reported in some crabapples. For instance, phlorizin, its isomer trilobatin, and their hydroxylated derivatives 3-hydroxyphlorizin and 3-hydroxytrilobatin were isolated from '*Red Splendor*' fruit. Due to the unique structure of dihydrochalcones compared to other flavonoids, the effect of alterations to chemical structure, such as the number and position of hydroxyl groups and glycosylation, on the antibacterial properties of dihydrochalcones might differ from other flavonoids.

In this study, we investigated the antibacterial effects of dihydrochalcones on 17 foodborne bacteria, including 12 Gram-negative and 5 Gram-positive bacteria, and determined the mechanisms. Dihydrochalcone compounds have similar structures and are well suited for studying the structure–antibacterial activity relationship.

2. Materials and methods

2.1. Chemicals, reagents, and microbial strains

Dihydrochalcone compounds, including phlorizin (phloretin-2′-*O*-glucoside, P2G), 3-hydroxyphlorizin (3-hydroxyphloretin-2′-*O*-glucoside, HP2G), trilobatin (phloretin-4′-*O*-glucoside, P4G), sieboldin (3-hydroxyphloretin-4′-*O*-glucoside, HP4G), phloretin (P), and 3-hydroxyphloretin (HP) (Fig. 1), were isolated as described by Xiao, *et al.* (2017)[6] with minor modifications. Briefly, one kilogram of *Malus* 'Winter Red' leaves were collected, frozen in liquid nitrogen, and then lyophilized using a vacuum freeze drier (ScanVac Coolsafe 110-4, LaboGene, Solrød Strand, Denmark). The lyophilized leaves were ground into powder, and then extracted three times with 80% ethanol (3 L) at room temperature for 24 h. After vacuum filtration using a sintered glass funnel with one layer of filter paper to remove the sediment, the supernatant was evaporated using a rotary evaporator (Senco Science and Technology Company, Shanghai, China) with the rotary speed at 100 rpm and the temperature at 55 °C for water bath and at −5 °C for cooling to obtain a viscous substance. Two liters of deionized water was added to the viscous substance, followed by ultrasonic vibration until the viscous substance was dispersed into turbid liquid. The turbid liquid was extracted three times with 0.9 L petroleum ether, followed by the extraction with 1.2 L ethyl acetate three times. The ethyl acetate fractions were combined and dried by evaporation to obtain the crude phenolic fraction, which was and then subjected to a custom-made open polyamide column chromatography (200–400 mesh, ∅ 9 × 40 cm). Different concentrations of methanol solution were used for elution in the sequences of 0% (1 L), 30% (2 L), 50% (2 L) and 80% (2 L). The fraction collected with the 80% methanol eluent was concentrated and subjected to a custom-made open Sephadex LH-20 column chromatography (∅ 3 × 120 cm) and eluted with methanol to obtain four fractions (F_1–F_4), based on HPLC analysis. Phlorizin was obtained by crystallization from F_2. F_3 was dried and re-dissolved in 100 mL of 30% methanol solution and then loaded onto a custom-made open SiliaSphere PC18 column (50 μm, ∅ 2.6 × 30 cm, the SiliaSphere PC18 packing was from SiliCycle, Quebec, Canada). After washing with 100 mL 30% methanol, the F_3 was eluted with step gradients of 40% (150 mL), 50% (150 mL) and 60% (150 mL) methanol to obtain three sub-fractions (F_{3-1}–F_{3-3}). The flow rate was approximately 3 mL min^{-1}. F_{3-1}, F_{3-2} and F_{3-3} were further purified by LC-20A liquid chromatography (Shimadzu Corporation, Tokyo, Japan) equipped with a FRC-10A automatic fraction collector and a photo-diode array detector to produce sieboldin, 3-hydroxyphlorizin, and trilobatin respectively. A YMC-Pack ODS-A column (5 μm, 10 mm × 250 mm, YMC CO., Ltd Kyoto, Japan) was used with a mobile phase of 50% methanol. After freeze drying, the four compounds were re-crystallized to increase their purities above 98%. To produce phloretin and 3-hydroxyphloretin, the purified phlorizin and sieboldin were dissolved in 50 mL of 4 M HCl solution and incubated in a water bath at 90 °C for 12 h, respectively. The hydrolysate was allowed to cool by standing at 4 °C for 4 h for crystallization, followed by centrifugation at 8000*g*. The insoluble compound was collected and washed three times in cold water and then re-dissolved in 100% methanol. The compounds were further purified by loading onto a custom-made Sephadex LH-20 column (∅ 1.6 × 120 cm, the LH-20 packing was from GE Healthcare BioSciences AB, Uppsala, Sweden) and eluted with methanol. The fraction containing phloretin or 3-hydroxyphloretin was collected based on the HPLC analysis, and then evaporated with nitrogen gas.

Mueller–Hinton broth (MHB) was purchased from Qingdao Hope Bio-Technology Co., Ltd (Qingdao, China). Fluorescein diacetate (FDA) and propidium iodide (PI) were obtained from Sigma-Aldrich (St Louis, MO, USA). The 12 Gram-negative bacteria analyzed in this study were *Pseudomonas fluorescens*

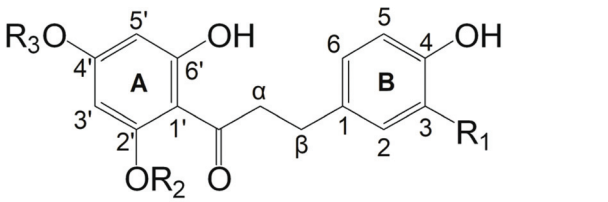

Phloretin : R1 = H, R2 = H, R3 = H
3-Hydroxyphloretin : R1 = OH, R2 = H, R3 = H
Phlorizin : R1 = H, R2 = glucoside, R3 = H
Trilobatin : R1 = H, R2 = H, R3 = glucoside
3-Hydroxyphlorizin : R1 = OH, R2 = glucoside, R3 = H
Sieboldin : R1 = OH, R2 = H, R3 = glucoside

Fig. 1 Chemical structures of dihydrochalcones.

BNCC 186286, *Klebsiella pneumoniae* BNCC 102997, *Escherichia coli* BNCC 133264, *Pseudomonas aeruginosa* BNCC 125486, *Proteus vulgaris* Hauser BNCC 336633, *Shigella dysenteriae* BNCC 103609, *Salmonella typhi* BNCC 108188, *Escherichia coli* (EHEC) O157:H7 BNCC 192101, *Yersinia enterocolitica* BNCC 186042, *Aeromonas hydrophila* BNCC 186123, *Alcaligenes faecalis* BNCC 102898, and *Serratia marcescens* BNCC 186186. The five Gram-positive bacteria analyzed in this study were *Listeria monocytogenes* BNCC 185986, *Bacillus cereus* BNCC 191738, *Enterococcus faecalis* BNCC 102668, *Micrococcus luteus* BNCC 102589, and *Staphylococcus aureus* BNCC 186335. All bacteria were purchased from BeNa Culture Collection (Suzhou, China). *L. monocytogenes* and *E. faecalis* were activated on tryptone soy agar (TSA), and all other bacteria were activated in nutrient agar (NA).

2.2. Antibacterial analysis of dihydrochalcone compounds

To evaluate the inhibition ratio of dihydrochalcone compounds on the growth of bacteria, the 17 activated bacterial strains were incubated in MHB overnight at 37 °C with constant shaking at 200 rpm. Bacterial culture concentration was adjusted to 3 McFarland (3×10^8 CFU mL^{-1}) and then diluted at a ratio of 1 : 300. After adding 0.2 or 0.4 mM P or HP, cultures were further incubated for 18 h. Bacterial cultures without dihydrochalcone treatment served as controls. After measuring the optical density (OD) at 600 nm using a microplate luminometer (Infinite® 200 Pro Tecan, Männedorf, Switzerland), the inhibition ratio was calculated by the following equation:

$$\text{Inhibition ratio} = (OD_{600control}\text{-}OD_{600treatment})/OD_{600control}.$$

The antibacterial activity of dihydrochalcone compounds in *M. luteus* and *K. pneumoniae* was evaluated as 50% minimal inhibitory concentration (MIC_{50}), which is defined as the concentration of compound required for 50% inhibition of bacterial growth. The MIC_{50} of each compound was determined according to the micro broth dilution method performed in 96-well microplates according to CLSI (Clinical and Laboratory Standards Institute, 2012).[28] Bacterial cultures at a concentration of $\sim 5 \times 10^5$ CFU per well were incubated for 18 h at 37 °C with constant shaking at 200 rpm. The dihydrochalcone concentration was 0.8 mM for P and HP or 3.2 mM for the other four compounds in the first well of the microplate, followed by 2-fold serial dilutions in the remaining wells.

The mutant prevention concentration (MPC) was estimated by determining the concentration that allowed recovery of no colony.[29] Bacterial cultures at a concentration of $>10^{10}$ CFU were spread onto agar plates containing a defined concentration of dihydrochalcones. In the preliminary studies, no obvious MPC was observed for the compounds such as P2G, P4G, HP2G and HP4G with their concentrations at 10 mM. So, the MPC was only assayed for P and HP in detail. Each strain was tested at 5 different dihydrochalcone concentrations (0, 0.75, 1.5, 3, 6 mM) at first, and then another concentration gradient (2, 3, 4, 5 mM). Plates were incubated at 37 °C for 48 h.

2.3. Morphological analysis

Suspensions of *M. luteus* or *K. pneumoniae* in logarithmic phase were centrifuged at 5000*g* for 10 min at 4 °C, and then washed 3 times with 100 mM phosphate buffer (pH 7.2). Washed cells were re-suspended in the same buffer with a final concentration of OD_{600} = 0.8, and incubated with or without P or HP at different concentrations at 37 °C for 5 h prior to morphological analysis.

For scanning electron microscopy (SEM) analysis, centrifuged precipitated cells were smeared on a one-ninth coverslip, aired to half-dry, and fixed in 2.5% (v/v) glutaraldehyde in PBS buffer at 4 °C overnight. After washing three times, cells were dehydrated sequentially in 30%, 50%, 70%, 80%, 90%, and 100% ethanol solutions. Finally, ethanol was replaced with isoamyl acetate. Samples were critical point dried (K850, Quorum, London, UK) and then sputter coated with gold under vacuum. They were then analyzed using a scanning electron microscope (S-4800, Hitachi, Tokyo, Japan) at 10.0 kV.

For transmission electron microscope (TEM) analysis, cells were centrifuged and pre-fixed in 2.5% (v/v) glutaraldehyde for 5 h at 4 °C, followed by low temperature agar embedding and fixation with 2.5% (v/v) glutaraldehyde at 4 °C for 12 h. Cells were then washed in the same buffer, dehydrated with gradient ethanol solutions, and post-fixed at 4 °C for 2 h with 1% osmic acid. Subsequently, samples were embedded in resin, sectioned on an ultramicrotome, stained with uranyl acetate and lead citrate, and observed by TEM (HT7700, Hitachi, Tokyo, Japan).

2.4. Protein content, inorganic phosphate content, cell membrane permeability, and respiration analyses

For protein content, inorganic phosphate content, and cell membrane permeability analyses, suspensions of *M. luteus* or *K. pneumoniae* in logarithmic phase were centrifuged at 5000*g* for 10 min at 4 °C and then washed 3 times with 0.85% normal saline. Washed cells were re-suspended in 0.85% normal saline and then incubated with or without P or HP at 37 °C for 5 h.

The supernatant protein concentration was determined by Bradford assay.[30] Briefly, 0.1 mL of supernatant and 3.9 mL of Coomassie Brilliant Blue G-250 reagent (J&K Scientific Ltd, Beijing, China) were mixed, left in the dark for 8 min, and then the absorbance was measured at 595 nm. The protein concentration was determined using a calibration curve prepared with bovine serum albumin.

To measure inorganic phosphate content, 700 μL of ascorbic acid-ammonium molybdate was added to 300 μL of supernatant, followed by incubation at 45 °C for 20 min. The absorbance was recorded at 660 nm.[31]

To check cell membrane permeability, the double-labeling with fluorescein diacetate (FDA) and propidium iodide (PI) live/dead staining assay was carried out according to Xing *et al.*[32] with minor modifications. FDA (dissolved in DMSO) and PI (dissolved in ddH_2O) were added to the suspensions at a final concentration of 10 μg mL^{-1} and 5 μg mL^{-1}, respect-

ively, then incubated in the dark. A BX63 fluorescence microscope (Olympus, Tokyo, Japan) was used to capture photographic images of stained cells. The excitation/emission wavelengths of FDA were 488/530 nm, and the excitation/emission wavelengths of PI were 493/636 nm. Heat-killed cells were used as a positive control, and untreated bacterial cells served as the negative control.

Bacterial cells for respiration rate measurement were prepared as described for cytochemical analysis. Respiration rate was measured with a liquid-phase oxygen electrode (Oxytherm, Hansatech, Norfolk, UK). Briefly, 400 μL of treated bacteria and 600 μL of 0.1 mM phosphate buffer (pH 7.2) were added to the reaction well. The magnetism rotor of the Oxytherm was spun at 35 rpm at room temperature.

2.5. Gene expression assay

Total RNA was extracted with Trizol reagent (Invitrogen, Carlsbad, CA, USA) following the manufacturer's instructions. First-strand cDNA was synthesized using the PrimeScript™ RT reagent Kit (Takara, Dalian, China), according to the manufacturer's protocol. All qRT-PCR experiments were performed with the Bio-Rad CFX96 system (Bio-Rad Laboratories, Hercules, CA, USA) with 0.1 mL 8-tube strips, using SYBR Premix Ex Taq™ II (Takara, Dalian, China). The housekeeping gene *16S rRNA* was used as the internal reference gene. The PCR amplification program was 95 °C for 3 min, 40 cycles of 95 °C for 10 s, and 60 °C for 30 s, followed by a melting curve analysis program. The primers for *16S rRNA*, *acpP* which encodes acyl carrier protein, *fabD* which encodes malonyl-CoA : ACP transacylase, *FabF* which encodes β-ketoacyl-ACP synthase, *fabG* which encodes β-ketoacyl-ACP reductase, *fabA* which encodes β-hydroxydecanoyl-ACP dehydratase, *fabZ* which encodes β-hydroxyacyl-ACP dehydratase, *cfa* which encodes cyclopropane fatty acyl phospholipid synthase, and *pspA* which encodes a peripheral membrane phage shock protein were shown in Table S1.†

2.6. Prediction of dihydrochalcone properties

The octanol/water distribution coefficient ($\log D$), which is used to represent molecule hydrophobicity and affinity of compounds for biological membranes,[33] was predicted for six dihydrochalcone compounds at pH 7.2 by ChemAxon MarvinSketch (2015.6.29, ChemAxon, Budapest, Hungary). Conformations were predicted using ChemBio3D Ultra 14 (CambridgeSoft, Waltham, MA, USA) after MM2 energy minimization.

2.7. Statistical analysis

All biochemical assays were performed on three independent days. On each day, three replicates were carried out. Data were expressed as means ± SE (n = 3). Analysis was performed using SPSS 12.0 (SPSS, Inc., Chicago, IL, USA).

3. Results

3.1. Antibacterial activity of dihydrochalcone compounds

Phloretin (P) and 3-hydroxyphloretin (HP) exhibited antibacterial effects on most bacterial strains that were analyzed, especially at a concentration of 0.4 mM, although the two compounds showed different antibacterial capacities (Table 1). Growth of *M. luteus* and *B. cereus* was almost completely inhibited by P at 0.4 mM, while inhibition was ~70% and ~85%, respectively, when treated with HP. The growth of *K. pneumoniae* was inhibited ~90% by HP at 0.4 mM, but only ~45% by P at the same concentration. The inhibition ratio was lower than 10% for *E. coli* (EHEC) O157:H7 and *S. dysenteriae*

Table 1 The inhibition ratio (%) of phloretin (P) and 3-hydroxyphloretin (HP) on the growth of 17 foodborne bacteria. Data are mean ± SE (n = 3)

Bacteria	P 0.2 mM	HP	P 0.4 mM	HP
Gram positive bacteria				
Staphylococcus aureus	48 ± 5 b	60 ± 3 ab	56 ± 5 ab	72 ± 3 a
Micrococcus luteus	35 ± 3 c	21 ± 5 d	93 ± 2 a	69 ± 4 b
Listeria monocytogenes	15 ± 6 d	30 ± 1 c	58 ± 3 a	49 ± 1 b
Bacillus cereus	— d	28 ± 3 c	96 ± 2 a	84 ± 1 b
Enterococcus faecalis	42 ± 2 ab	22 ± 2 c	38 ± 3 b	47 ± 3 a
Gram negative bacteria				
Klebsiella pneumonia	25 ± 1 d	36 ± 5 c	46 ± 1 b	89 ± 4 a
Alcaligenes faecalis	— c	17 ± 2 b	37 ± 4 a	38 ± 8 a
Escherichia coli EHEC O157:H7	— b	— b	— b	17 ± 4 a
Yersinia enterocolitica	16 ± 1 b	17 ± 1 b	44 ± 5 a	51 ± 1 a
Salmonella typhi	27 ± 2 b	39 ± 4 ab	35 ± 2 ab	50 ± 7 a
Proteus vulgaris Hauser	14 ± 4 c	17 ± 2 c	30 ± 1 b	49 ± 2 a
Serratia marcescens	— b	— b	35 ± 7 a	34 ± 8 a
Aeromonas hydrophila	22 ± 3 b	23 ± 2 b	52 ± 5 a	25 ± 1 b
Pseudomonas fluorescens	— b	— b	13 ± 7 a	— ab
Pseudomonas aeruginosa	— b	— b	14 ± 4 a	— ab
Shigella dysenteriae	— b	— b	— b	40 ± 7 a
Escherichia coli	— c	— c	23 ± 4 b	39 ± 4 a

"—" indicates inhibition ratio < 10. Different letters indicate significant difference at $P < 0.05$.

when treated with P and for *P. fluorescens* and *P. aeruginosa* when treated with HP.

As Gram-positive *M. luteus* and Gram-negative *K. pneumoniae* were very sensitive but showed different sensitivities to P and HP treatments, these two strains were used for further studies to clarify the antibacterial mechanisms of dihydrochalcones.

To explore the relationship between compound structure and antibacterial activity, P and HP, as well as their glycosylated derivatives (phloretin-2′-*O*-glucoside, P2G; 3-hydroxyphloretin-2′-*O*-glucoside, HP2G; phloretin-4′-*O*-glucoside, P4G; and 3-hydroxyphloretin-4′-*O*-glucoside, HP4G), were analyzed against these two strains (Table 2). Compared to HP, P showed a lower MIC_{50} for *M. luteus* (around 0.2 mM), but a higher MIC_{50} for *K. pneumoniae* (around 0.4 mM). However, both P and HP had significantly lower MIC_{50} values compared to their glycosylated derivatives (P2G, P4G, HP2G, and HP4G). Moreover, compared to compounds glycosylated at the 4′-position (P4G and HP4G), those glycosylated at the 2′-position (P2G and HP2G) exhibited significantly higher MIC_{50} values against both bacteria.

The MPC values of both P and HP were 4 mM for *K. pneumoniae* and 3 mM for *M. luteus* (Table 3).

Table 2 MIC_{50} values for six dihydrochalcone compounds. Data are mean ± SE (n = 3)

Bacteria	P	HP	P2G	HP2G	P4G	HP4G
K. pneumonia	0.41 ± 0.04 b	0.30 ± 0.03 a	—d	—d	2.40 ± 0.11 c	2.23 ± 0.06 c
M. luteus	0.23 ± 0.03 a	0.32 ± 0.04 b	—e	—e	3.35 ± 0.50 d	1.48 ± 0.26 c

MIC_{50} is the concentration (mM) of compound that results in 50% inhibition of bacterial growth; "—" indicates no obvious antibacterial effects were observed at the maximum concentration of 3.2 mM. Different letters indicate significant difference at $P < 0.05$. P, phloretin; HP, 3-hydroxyphloretin; P2G, phlorizin, phloretin-2′-glucoside; HP2G, 3-hydroxyphloretin-2′-glucoside; P4G, trilobatin, phloretin-4′-glucoside; HP4G, sieboldin, 3-hydroxyphloretin-4′-glucoside.

Table 3 MPC values for six dihydrochalcone compounds

Bacteria	P	HP	P2G	HP2G	P4G	HP4G
K. pneumonia	4	4	—	—	—	—
M. luteus	3	3	—	—	—	—

MPC is the mutant prevention concentration (mM). "—" indicates no obvious MPC was observed at the concentration of 10 mM. P, phloretin; HP, 3-hydroxyphloretin; P2G, phlorizin, phloretin-2′-glucoside; HP2G, 3-hydroxyphloretin-2′-glucoside; P4G, trilobatin, phloretin-4′-glucoside; HP4G, sieboldin, 3-hydroxyphloretin-4′-glucoside.

3.2. Morphological, biochemical, molecular and physiological changes in bacteria induced by dihydrochalcone compound treatment

To further explore the antibacterial mechanisms of dihydrochalcones, *M. luteus* and *K. pneumoniae* were treated with P and HP at the MIC_{50} concentration for P (0.2 mM for *M. luteus*, and 0.4 mM for *K. pneumoniae*) or double MIC_{50}.

SEM revealed that without treatment (Fig. 2A), the shape of *K. pneumoniae* was short and rod-like, and the cell surface was intact and smooth without damage. Cells treated with P became crepey and agminated (Fig. 2B). After treatment with HP (Fig. 2C), cells became flat and cell membranes were not well defined. Moreover, some cells had a wizened appearance. An increase in P or HP concentration increased cellular damage, which was easily discerned (Fig. 2D and E). For *M. luteus*, untreated cells were even and plump (Fig. 2F). Cells treated with relatively lower concentrations of P and HP (Fig. 2G and H) were unaltered. However, higher concentrations of HP (Fig. 2J) induced bubble-like protuberances, while higher concentrations of P (Fig. 2I) caused cells to form irregularly shaped fragments.

Control groups showed uniform cellular structure and homogeneous intracellular microstructure (Fig. 3A and F). After treatment, *K. pneumoniae* exhibited significant interior damage and leakage of intracellular components (Fig. 3B–E). *M. luteus* exhibited a similar appearance after treatment and

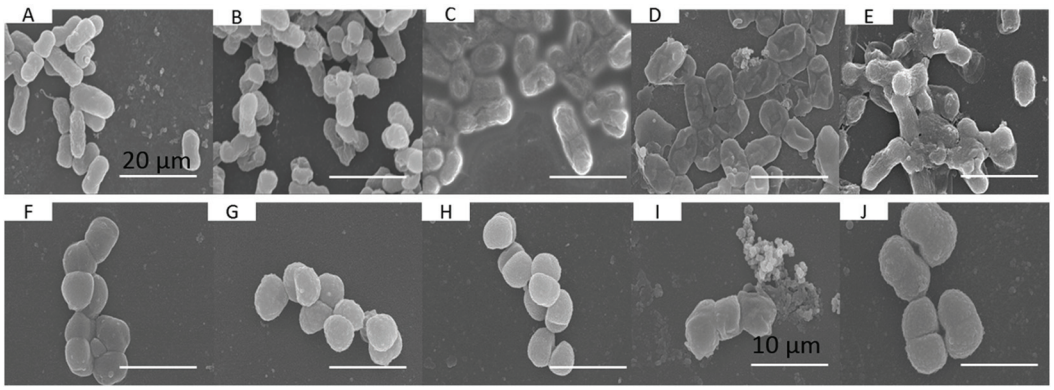

Fig. 2 The morphological structure of bacterial cells with or without phloretin (P) and 3-hydroxyphloretin (HP) treatment. *K. pneumoniae*: A, Control; B and C, 0.4 mM P and HP; D and E, 0.8 mM P and HP. *M. luteus*: F, Control; G and H, 0.2 mM P and HP; I and J, 0.4 mM P and HP. Scale bar of A–H, 20 μm; scale bar of I and J, 10 μm.

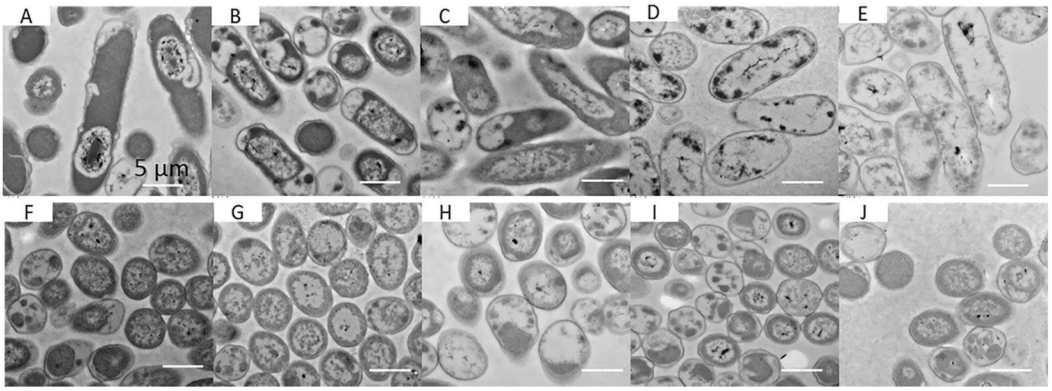

Fig. 3 The ultrastructure of bacterial cells with or without phloretin (P) and 3-hydroxyphloretin (HP) treatment. *K. pneumoniae*: A, Control; B and C, 0.4 mM P and HP; D and E, 0.8 mM P and HP. *M. luteus*: F, Control; G and H, 0.2 mM P and HP; I and J, 0.4 mM P and HP. Scale bar of A–J, 5 μm.

cells became hollow (Fig. 3G–J) after leakage, but overall cellular damage was reduced compared to the damage observed in *K. pneumoniae.*

To determine if the antibacterial effects of P and HP involved permeabilization of the plasma membrane, the cell viability assay employed two well-known dyes, membrane-impermeant PI (binding with DNA and exhibiting fluorescence) in combination with the membrane-permeant FDA (exhibiting fluorescence upon cleavage by cell esterases). Clearly, most cells of the negative control emitted green fluorescence of FDA, indicating that they were alive (Fig. 4A and G). In contrast, almost all cells of the positive control (heat killed at 100 °C for 20 min) presented strong red fluorescence of PI, indicating that they were dead cells with disrupted membranes (Fig. 4B and H). Following treatment with P or HP and the increases in compound concentrations, the number of reactive cells (with green fluorescence) decreased while that of dead cells (with red fluorescence) increased (Fig. 4C–F and I–N). Moreover, it was found that P showed a greater effect on *M. luteus* and less pronounced effect on *K. pneumoniae* compared to HP.

After treatment with P or HP, both protein and inorganic phosphate leakage increased significantly (Fig. 5A). However, the two compounds showed different effects on protein leakage. Compared to P, HP exhibited a reduced effect on *M. luteus*, but a significantly greater effect on *K. pneumoniae*. Inorganic phosphate leakage became more severe after treatment, especially with P treatment in both strains (Fig. 5B).

The modification of fatty acids in bacterial membranes might relate to the regulation of genes in the type II fatty acid synthase systems. In this study, the expression levels of membrane fatty acid biosynthesis-associated genes including *acpP* which encodes acyl carrier protein (ACP), *fabD* which encodes malonyl-CoA : ACP transacylase, *Fab*F which encodes β-ketoacyl-ACP synthase, *fabG* which encodes β-ketoacyl-ACP reductase, *fabA* which encodes β-hydroxydecanoyl-ACP dehydratase, *fabZ* which encodes β-hydroxyacyl-ACP dehydratase, *cfa* which encodes cyclopropane fatty acyl phospholipid synthase, and *pspA* which encodes a peripheral membrane phage shock protein were assayed (Fig. 6). It was found that the expression levels of *fabG*, *fabA* and *fabZ* in *K. pneumoniae* did not change after higher concentrations of P and HP treatments, but decreased after lower chemical concentration treatments. The expression of *cfa* did not change after treated with P treatment, but significantly decreased with HP treatment. Levels of *pspA* did not change after HP treatment, but increased after P treatment, especially with higher concentration of P (Fig. 6A). For *M. luteus*, the expression level of *acpP* did not change after the treatments, except that it increased with the treatment of higher concentration of P. The levels of *fabD*, *fabF*, *fabG* and *fabA* remained unchanged after treated with P. However, with HP treatment the levels of *fabD* and *fabG* increased while that of *fabF* decreased (Fig. 6B).

The lower concentration of P and HP had no effect on the respiration of *M. luteus*, but decreased respiration in *K. pneumoniae* (Fig. 7). At two times the lower concentration, both P and HP significantly inhibited *M. luteus* respiration, and *K. pneumoniae* respiration was decreased even further. The effects of the two compounds on the respiration of the two bacteria were similar.

3.4 The predicted properties of dihydrochalcone compounds

The octanol/water distribution coefficient ($\log D$), which is used to represent molecule hydrophobicity and affinity of compounds for biological membranes,[33] was predicted for six dihydrochalcone compounds at pH 7.2 using software. The values of $\log D$ were ordered as follows: P > HP > P4G > HP4G > P2G > HP2G (Table 4). Conformations of the compounds were also predicted. It was found that the minimum energy conformations of P and HP were very similar. Glycosylation at the 2′-position changed the minimum energy conformations of P and HP more significantly than glycosylation at the 4′-position.

4. Discussion

The cell wall of Gram-positive bacteria consists of a thick peptidoglycan layer, whereas that of Gram-negative bacteria consists of a thinner peptidoglycan layer and an outer lipid membrane

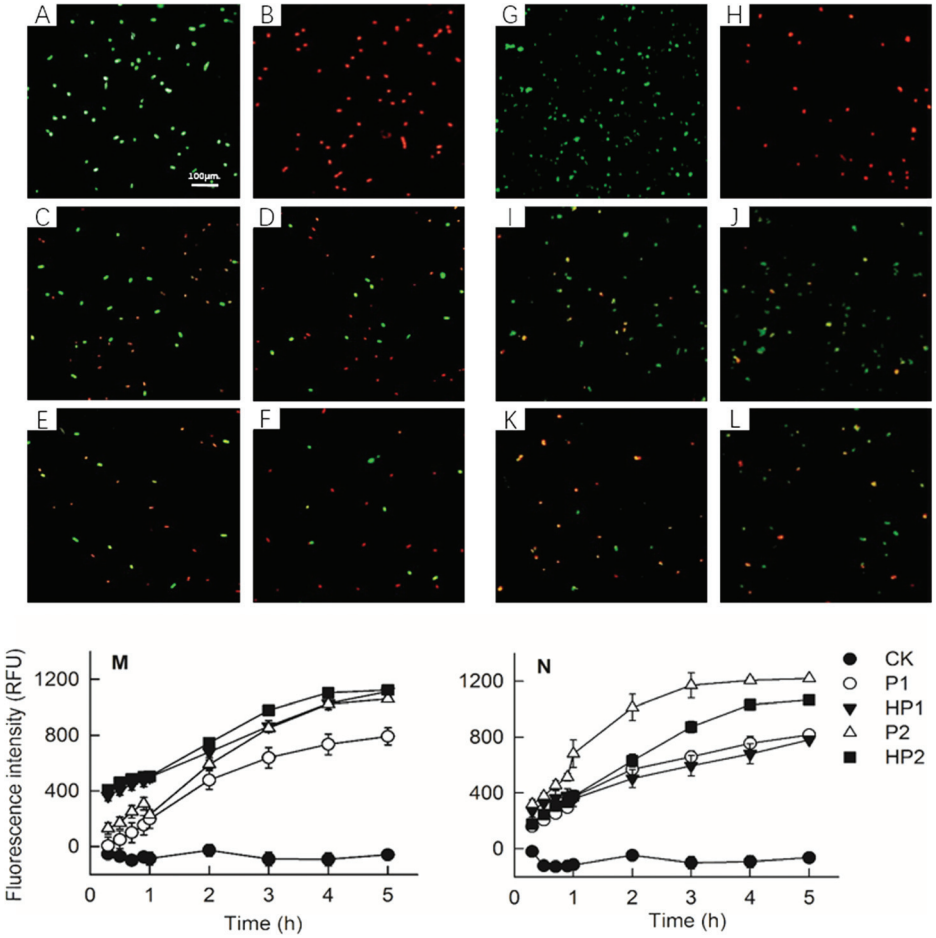

Fig. 4 Cells viability by double-staining with fluorescein diacetate (FDA, green fluorescence) and propidium iodide (PI, red fluorescence). *K. pneumoniae*: A, untreated cells; B, heat-killed cells; C and D, 0.4 mM phloretin (P) and 3-hydroxyphloretin (HP) treatments for 5 hours; E and F, 0.8 mM P and HP treatments for 5 hours; M, PI fluorescence with differently treated time. *M. luteus*: G, untreated cells; H, heat-killed cells; I and J, 0.2 mM P and HP treatments for 5 hours; K and L, 0.4 mM P and HP treatments for 5 hours; N, PI fluorescence with differently treated time. In panel M and N, CK means control; P1 and HP1 indicates 0.2 mM of P or HP for *M. luteus*, and 0.4 mM of P or HP for *K. pneumoniae*; P2 and HP2 indicates 0.4 mM of P or HP for *M. luteus*, and 0.8 mM of P or HP for *K. pneumoniae*. Data are mean ± SE (n = 3).

containing lipopolysaccharide. In addition, there are multiple porins and efflux pumps on the Gram-negative bacteria surface, which prevent small molecule compounds from reaching intracellular targets and accumulating in bacterial cells.[34] Due to their different cell wall structures, it was suggested that flavonoids exert better antibacterial activity against Gram-positive strains compared to Gram-negative strains.[18,20] However, this study showed that dihydrochalcones had excellent antibacterial effects on both Gram-positive bacteria, such as *M. luteus* and *B. cereus*, and Gram-negative bacteria, such as *K. pneumoniae* (Tables 1 and 2, Fig. 2 and 3). Heather extract, which mainly contains epicatechin dimers and trimers, also causes greater inhibition in *K. pneumoniae* than in Gram-positive bacteria.[35] Moreover, glycosylation at the A-ring of dihydrochalcones, especially at the 2′-position, played a key role in antibacterial activity (Table 2).

Glycosylation can potentially decrease the hydrophobicity of a molecule. Low hydrophobicity leads to increased potential for aggregation around a lipid membrane polar head and difficulty interacting with the hydrophobic bilayer core, which is sensitive to perturbation.[36] Indeed, the hydrophobicity of trilobatin and 3-hydroxytrilobatin was higher than that of phlorizin and 3-hydroxyphlorizin (Table 4). Thus hydrophobicity was altered by glycosylation at different positions and might have the greatest effect on antibacterial properties of dihydrochalcones. In addition, a linear conformation was thought to assist diffusion through the phospholipid bilayer and alter bilayer properties to a greater extent.[37,38] For instance, the linearly shaped molecules quercetin and luteolin destabilize the lipid membrane and make it more rigid.[39] According to the minimized energy conformation skeletons evaluated using Chem3D (Table 4), trilobatin and 3-hydroxytrilobatin showed approximately plane structures similar to the aglycones, whereas the two rings of phlorizin and 3-hydroxyphlorizin were not planar due to the flexible C_3 chain. The effect of glycosylation on conformation might be another way that glycosylation affects the antibacterial capacity of dihydrochalcones.

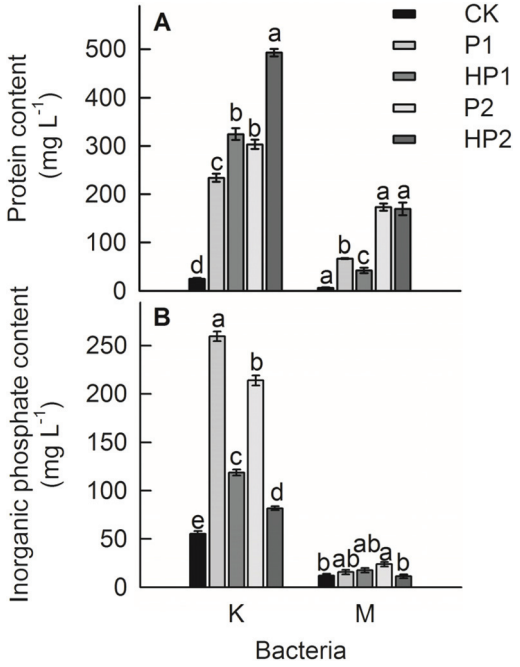

Fig. 5 Protein leakage (A) and inorganic phosphate leakage (B) in bacteria (K, *K. pneumoniae*; M, *M. luteus*) with or without phloretin (P) and 3-hydroxyphloretin (HP) treatment. P1, HP1, 0.2 mM for M, and 0.4 mM for K; P2, HP2, 0.4 mM for M, and 0.8 mM for K. Data are mean ± SE (n = 3). Different letters indicate significant difference at $P < 0.05$.

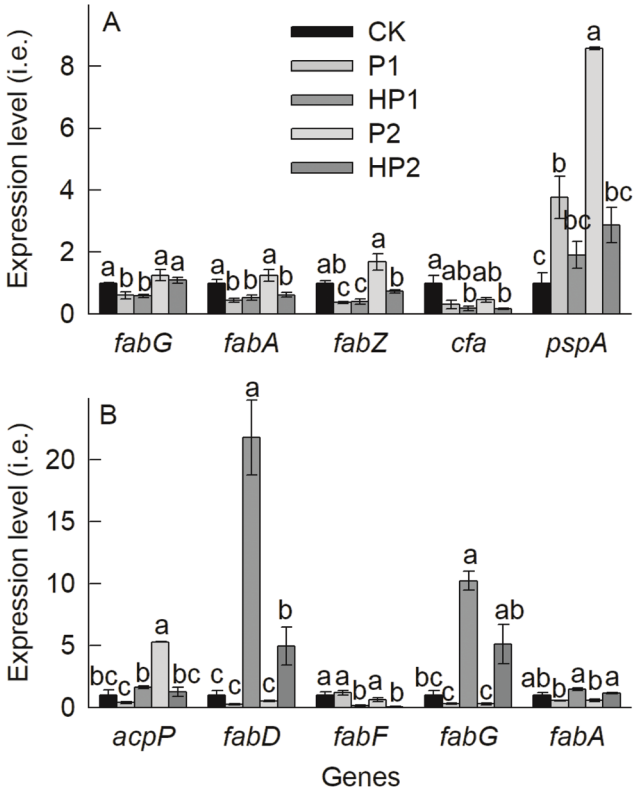

Fig. 6 Relative expression levels of genes involved in fatty acids biosynthesis in bacteria (panel A, *K. pneumoniae*; panel B, *M. luteus*) with or without phloretin (P) and 3-hydroxyphloretin (HP) treatment. P1, HP1, 0.2 mM for M, and 0.4 mM for K; P2, HP2, 0.4 mM for M, and 0.8 mM for K. Data are mean ± SE (n = 3). Different letters indicate significant difference at $P < 0.05$. *fabG*, encoding β-ketoacyl-ACP reductase; *fabA*, encoding β-hydroxydecanoyl-ACP dehydratase; *fabZ*, encoding β-hydroxyacyl-ACP dehydratase; *cfa*, encoding cyclopropane fatty acyl phospholipid synthase; *pspA*, encoding a peripheral membrane phage shock protein, *acpP*, encoding acyl carrier protein; *fabD*, encoding malonyl-CoA : ACP transacylase; *FabF*, encoding β-ketoacyl-ACP synthase.

Similar to flavonoids such as quercetin and kaempferol, which may alter cell membrane properties including fluidity,[19] dihydrochalcones might also inhibit growth of both Gram-positive and Gram-negative strains by affecting the cell membrane. This mode of inhibition is supported by the increased membrane permeability and leakage of both protein and inorganic phosphate observed in this study (Fig. 2–5). As the expression levels of membrane fatty acids biosynthesis-associated genes did not correlate with the damage levels of membrane with different dihydrochalcone treatments (Fig. 6), the transcription process of these genes might not be the major target of dihydrochalcones. The pronounced increases in the expression levels of *pspA* in *K. pneumoniae* with P treatments and that of *fabD* and *fabG* in *M. luteus* with HP treatment might be a positive feedback of bacteria to the treatments, to reduce the damage as possibly. Indeed, the expressions of membrane fatty acids biosynthesis-associated genes was also found to be increased in *E. coli* and *S. aureus* when treated with naringenin.[8] The increased protein (bio-macromolecule) leakage and reduced inorganic phosphate (small molecule) leakage after treatment with 3-hydroxyphloretin compared to phloretin suggests that these compounds have different antibacterial mechanisms. Specifically, the hydroxyl group at the 3-position of the B-ring played a key role in the antibacterial mechanism of dihydrochalcones, which is also supported by MIC_{50} values (Table 2). After treatment at the MIC_{50} value, respiration of *M. luteus* did not change, but membrane permeability increased significantly (Fig. 5 and 7). Therefore,

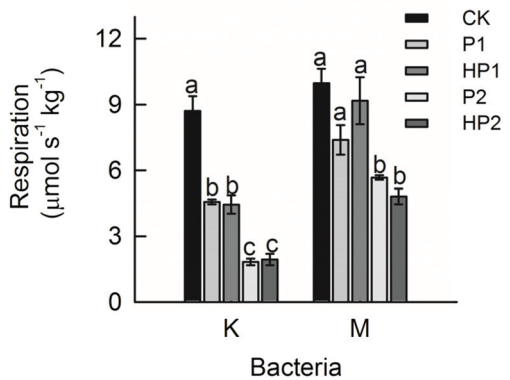

Fig. 7 Bacterial (K, *K. pneumoniae*; M, *M. luteus*) respiration with or without phloretin (P) and 3-hydroxyphloretin (HP) treatment. P1, HP1, 0.2 mM for M, and 0.4 mM for K; P2, HP2, 0.4 mM for M, and 0.8 mM for K. Data are mean ± SE (n = 3). Different letters indicate significant difference at $P < 0.05$.

Table 4 Molecular properties of six dihydrochalcone compound skeletons

Compounds	log D^a	Conformation[b]
P	3.83	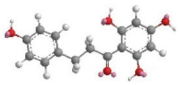
HP	3.52	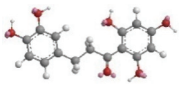
P2G	0.89	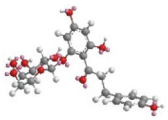
HP2G	0.59	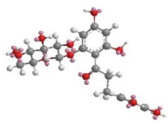
P4G	1.62	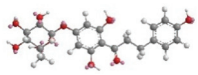
HP4G	1.31	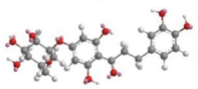

[a] log D indicates the molecule hydrophobicity and affinity of compounds for biological membranes, skeleton hydrophobicity was calculated at pH 7.2. [b] Conformation after MM2 energy minimization (0.01 RMS gradient). P, phloretin; HP, 3-hydroxyphloretin; P2G, phlorizin, phloretin-2′-glucoside; HP2G, 3-hydroxyphloretin-2′-glucoside; P4G, trilobatin, phloretin-4′-glucoside; HP4G, sieboldin, 3-hydroxyphloretin-4′-glucoside.

dihydrochalcones damage the membrane first and then affect respiration in *M. luteus*. However, damage to the membrane and respiration might occur simultaneously in *K. pneumoniae*, suggesting that the antibacterial mechanism of dihydrochalcones also depends on the strain type.

It was reported that the mutant prevention concentration (MPC) of ciprofloxacin for urinary tract infection isolates of *Escherichia coli* was 0.1–5 mg L^{-1},[29] whereas that of fluoroquinolone for *Mycobacterium smegmatis* was 0.9–19 mg L^{-1}.[40] Compared to the antibiotics, P and HP showed much higher MPC values (800–1200 mg L^{-1}, Table 3), which might limit the application of the chemicals. However, as the most abundant natural flavonoids in *Malus*,[6] dihydrochalcones still have great potential utilization in the food industry as additives.

5. Conclusion

In general, dihydrochalcones had excellent antibacterial effects on both Gram-positive and Gram-negative bacteria. Both glycosylation at the 2′-position of the A-ring and hydroxyl group at the 3-position of the B-ring played a key role in the antibacterial activity of dihydrochalcones. Within a certain range, the hydrophobicity of dihydrochalcones might be positively correlated with their antibacterial activity. The antibacterial mechanism of dihydrochalcones was mainly through damage to the cell membrane. However, the antibacterial mechanism also depended on strain type. This study elucidated the broad-spectrum antibacterial properties of dihydrochalcone compounds commonly found in the genus *Malus* against foodborne pathogens, as well as the antibacterial mechanisms. It provides theoretical guidance for future research and application of dihydrochalcones in the food industry.

Conflicts of interest

There are no conflicts to declare.

Acknowledgements

This study was supported by the National Key R&D Program of China (2018YFD1000200) and the National Nature Science Foundation of China (31972366).

References

1 C. S. Buer, F. Kordbacheh, T. T. Truong, C. H. Hocart and M. A. Djordjevic, Alteration of flavonoid accumulation patterns in transparent *testa* mutants disturbs auxin transport, gravity responses, and imparts long-term effects on root and shoot architecture, *Planta*, 2013, **238**, 171–189.
2 M. M. Petkovsek, F. Stamper and R. Veberic, Parameters of inner quality of the apple scab resistant and susceptible apple cultivars (*Malus domestica Borkh.*), *Sci. Hortic.*, 2007, **114**, 37–44.
3 J. M. Watkins, J. M. Chapman and G. K. Muday, Abscisic acid-induced reactive oxygen species are modulated by flavonols to control stomata aperture, *Plant Physiol.*, 2017, **175**, 1807–1825.
4 S. Masumoto, Y. Akimoto, H. Oike and M. Kobori, Dietary phloridzin reduces blood glucose levels and reverses SGLT1 expression in the small intestine in streptozotocin-induced diabetic mice, *J. Agric. Food Chem.*, 2009, **57**, 4651–4656.
5 T. D. D. Bernonville, S. Guyot, J. P. Paulin, M. Gaucher, L. Loufrani, D. Henrion, S. Derbré, D. Guilet, P. Richomme, J. F. Dat and M. N. Brisset, Dihydrochalcones: Implication in resistance to oxidative stress and bioactivities against advanced glycation end-products and vasoconstriction, *Phytochemistry*, 2010, **71**, 443–452.
6 Z. Xiao, Y. Zhang, C. Xian, Y. Wang, W. Chen, Q. Xu, P. Li and F. Ma, Extraction, identification, and antioxidant and anticancer tests of seven dihydrochalcones from *Malus* 'Red Splendor' fruit, *Food Chem.*, 2017, **231**, 324–331.
7 U. Takahama and S. Hirota, Interactions of flavonoids with α-amylase and starch slowing down its digestion, *Food Funct.*, 2018, **9**, 677–687.
8 L. H. Wang, X. A. Zeng, M. S. Wang, C. S. Brennan and D. Gong, Modification of membrane properties and fatty acids biosynthesis-related genes in *Escherichia coli* and

Staphylococcus aureus: Implications for the antibacterial mechanism of naringenin, *Biochim. Biophys. Acta, Biomembr.*, 2017, **1860**, 481–490.

9 C. M. Peixoto, M. I. Dias, M. J. Alves, R. C. Calhelha, L. Barros, S. P. Pinho and I. C. F. R. Ferreira, Grape pomace as a source of phenolic compounds and diverse bioactive properties, *Food Chem.*, 2018, **253**, 132–138.

10 Z. Tao, W. Jin, M. Ao, S. Zhai, H. Xu and L. Yu, Evaluation of the anti-inflammatory properties of the active constituents in *Ginkgo biloba* for the treatment of pulmonary diseases, *Food Funct.*, 2019, **10**, 2209–2220.

11 C. Rodriguez-Perez, R. Quirantes-Pine, J. Uberos, C. Jimenez-Sanchez, A. Peña and A. Segura-Carretero, Antibacterial activity of isolated phenolic compounds from cranberry (*Vaccinium macrocarpon*) against *Escherichia coli*, *Food Funct.*, 2016, **7**, 1564–1573.

12 A. C. D. Camargo, G. B. Rasera, L. D. P. Silva, V. O. Alvarenga, A. S. Sant'Ana and F. Shahidi, Phenolic acids and flavonoids of peanut by-products: Antioxidant capacity and antimicrobial effects, *Food Chem.*, 2017, **237**, 538–544.

13 H. Ikigai, T. Nakae, Y. Hara and T. Shimamura, Bactericidal catechins damage the lipid bilayer, *Biochim. Biophys. Acta, Biomembr.*, 1993, **1147**, 132–136.

14 A. Mori, C. Nishino, N. Enoki and S. Tawata, Antibacterial activity and mode of action of plant flavonoids against *Proteus vulgaris* and *Staphylococcus aureus*, *Phytochemistry*, 1987, **26**, 2231–2234.

15 A. Plaper, M. Golob, I. Hafner, M. Oblak, T. Solmajer and R. Jerala, Characterization of quercetin binding site on DNA gyrase, *Biochem. Biophys. Res. Commun.*, 2003, **306**, 530–536.

16 D. Barreca, E. Bellocco, G. Laganà, G. Ginestra and C. Bisignano, Biochemical and antimicrobial activity of phloretin and its glycosilated derivatives present in apple and kumquat, *Food Chem.*, 2014, **160**, 292–297.

17 L. E. Alcaráz, S. E. Blanco, O. N. Puig, F. Tomás and F. H. Ferretti, Antibacterial activity of flavonoids against methicillin-resistant *Staphylococcus aureus* strains, *J. Theor. Biol.*, 2000, **205**, 231–240.

18 H. P. Ávila, E. F. A. Smânia, F. D. Monache and A. S. Júnior, Structure-activity relationship of antibacterial chalcones, *Bioorg. Med. Chem.*, 2008, **16**, 9790–9794.

19 T. Wu, M. He, X. Zang, Y. Zhou, T. Qiu, S. Pan and X. Xu, A structure–activity relationship study of flavonoids as inhibitors of *E. coli* by membrane interaction effect, *Biochim. Biophys. Acta, Biomembr.*, 2013, **1828**, 2751–2756.

20 Y. Xie, W. Yang, F. Tang, X. Chen and L. Ren, Antibacterial activities of flavonoids: structure-activity relationship and mechanism, *Curr. Med. Chem.*, 2015, **22**, 132–149.

21 R. Tsao, R. Yang, J. C. Young and H. Zhu, Polyphenolic profiles in eight apple cultivars using high-performance liquid chromatography (HPLC), *J. Agric. Food Chem.*, 2003, **51**, 6347–6353.

22 Y. P. Lin, F. L. Hsu, C. S. Chen, J. W. Chern and M. H. Lee, Constituents from the Formosan apple reduce tyrosinase activity in human epidermal melanocytes, *Phytochemistry*, 2007, **68**, 1189–1199.

23 C. S. Chen, D. Zhang, Y. Q. Wang, P. M. Li and F. W. Ma, Effects of fruit bagging on the contents of phenolic compounds in the peel and flesh of 'Golden Delicious', 'Red Delicious', and 'Royal Gala' apples, *Sci. Hortic.*, 2012, **142**, 68–73.

24 I. Pontais, D. Treutter, J. P. Paulin and M. N. Brisset, *Erwinia amylovora* modifies phenolic profiles of susceptible and resistant apple through its type III secretion system, *Physiol. Plant.*, 2008, **132**, 262–271.

25 M. Leopoldini, N. Russo and M. Toscano, The molecular basis of working mechanism of natural polyphenolic antioxidants, *Food Chem.*, 2011, **125**, 288–306.

26 Z. Xiao, Y. Wang, J. Wang, P. Li and F. Ma, Structure-antioxidant capacity relationship of dihydrochalcone compounds in *Malus*, *Food Chem.*, 2019, **275**, 354–360.

27 J. R. Dimmock, D. W. Elias, M. A. Beazely and N. M. Kandepu, Bioactivities of chalcones, *Curr. Med. Chem.*, 1999, **6**, 1125–1149.

28 CLSI, *Methods for dilution antimicrobial susceptibility tests for bacteria that grow aerobically; Approved standard–ninth edition*, CLSI Document M07-A9, Clinical and Laboratory Standards Institute, Wayne, PA, USA, 2012.

29 L. L. Marcusson, S. K. Olofsson, P. K. Lindgren, O. Cars and D. Hughes, Mutant prevention concentrations of ciprofloxacin for urinary tract infection isolates of *Escherichia coli*, *J. Antimicrob. Chemother.*, 2005, **55**, 938–943.

30 E. Harlow and D. Lane, Bradford assay, *Cold Spring Harb. Protoc.*, 2006, DOI: 10.1101/pdb.prot4644.

31 B. N. Ames, Assay of inorganic phosphate, total phosphate and phosphatases, *Methods Enzymol.*, 1966, **8**, 115–118.

32 K. Xing, Y. Xing, Y. Liu, Y. Zhang, X. Shen, X. Li, X. Miao, Z. Feng, X. Peng and S. Qin, Fungicidal effect of chitosan via inducing membrane disturbance against *Ceratocystis fimbriata*, *Carbohydr. Polym.*, 2018, **192**, 95–103.

33 G. Nellie, Z. Alexander, L. Pamela, C. Michael, M. C. Oliver, C. Arnon, K. Victor and Z. Boris, Relative hydrophobicity and lipophilicity of drugs measured by aqueous two-phase partitioning, octanol-buffer partitioning and HPLC. A simple model for predicting blood-brain distribution, *Eur. J. Med. Chem.*, 2003, **38**, 391–396.

34 M. F. Richter, B. S. Drown, A. P. Riley, A. Garcia, T. Shirai, R. L. Svec and P. J. Hergenrother, Predictive compound accumulation rules yield a broad-spectrum antibiotic, *Nature*, 2017, **545**, 299–304.

35 C. B. Van Buiten, N. H. Yennawar, C. N. Pacheco, E. Hatzakis and R. J. Elias, Physicochemical interactions with (−)-epigallocatechin-3-gallate drive structural modification of celiac-associated peptide α_2-gliadin (57–89) at physiological conditions, *Food Funct.*, 2019, **10**, 2997–3007.

36 H. A. Scheidt, A. Pampel, L. Nissler, R. Gebhardt and D. Huster, Investigation of the membrane localization and distribution of flavonoids by high-resolution magic angle spinning NMR spectroscopy, *Biochim. Biophys. Acta, Biomembr.*, 2004, **1663**, 97–107.

37 O. Wesolowska, J. Gasiorowska, J. Petrus, B. Czarnik-Matusewicz and K. Michalak, Interaction of prenylated chalcones and flavanones from common hop with phosphatidylcholine model membranes, *Biochim. Biophys. Acta, Biomembr.*, 2014, **1838**, 173–184.

38 M. Huang, E. Su, F. Zheng and C. Tan, Encapsulation of flavonoids in liposomal delivery systems: the case of quercetin, kaempferol and luteolin, *Food Funct.*, 2017, **8**, 3198–3208.

39 A. B. Hendrich, R. Malon, A. Pola, Y. Shirataki, N. Motohashi and K. Michalak, Differential interaction of Sophora isoflavonoids with lipid bilayers, *Eur. J. Pharm. Sci.*, 2002, **16**, 201–208.

40 G. Sindelar, X. Zhao, A. Liew, Y. Dong, T. Lu, J. Zhou, J. Domagala and K. Drlica, Mutant prevention concentration as a measure of fluoroquinolone potency against mycobacteria, *Antimicrob. Agents Chemother.*, 2000, **44**, 3337–3343.